Folded phonons in $(GaAs)_{n_1}/(AlAs)_{n_2}$ superlattices grown along the [012] direction

Z. V. Popović,* H. J. Trodahl,† and M. Cardona
Max-Planck-Institut für Festkörperforschung, Heisenbergstrasse 1, Postfach 80 06 65, D-7000 Stuttgart 80, Federal Republic of Germany

E. Richter and D. Strauch
Institut für Theoretische Physik, Universität Regensburg, D-8400 Regensburg, Federal Republic of Germany

K. Ploog
Max-Planck-Institut für Festkörperforschung, Heisenbergstrasse 1, Postfach 80 06 65, D-7000 Stuttgart 80, Federal Republic of Germany

(Received 31 January 1989)

We present Raman scattering data for folded acoustic phonons in GaAs/AlAs superlattices grown along the [012] direction. Doublets of mixed transverse and longitudinal character, with the selection rules predicted by symmetry, are clearly observed. The frequencies of the observed modes are not fully in agreement with calculations based on the continuum model.

Raman scattering by the folded acoustic-phonon branches of superlattices is now routinely observed (for a review, see Ref. 1). To date, measurements have been restricted to superlattices grown on high-symmetry planes, of which the most common are (001)-oriented superlattices of GaAs/AlAs, probably because of difficulties in preparing high-quality samples on low-symmetry substrates. For (001) superlattices, only the longitudinal acoustic branch is Raman active in backscattering; clear observations of scattering by a transverse acoustic branch have not yet been reported. In this paper we present data on Raman scattering by folded phonons in (012)-oriented GaAs/AlAs superlattices and demonstrate that in this case one of the TA branches can be observed.

The propagation of acoustic waves in cubic solids is well known.[2] Here we consider propagation with the wave vector in the (y,z) plane, for which the velocities are[2]

$$V_T=(C_{44}/\rho)^{1/2}\,, \tag{1}$$

$$V_{QT}=[(C_{11}+C_{44}-D)/(2\rho)]^{1/2}\,, \tag{2}$$

$$V_{QL}=[(C_{11}+C_{44}+D)/(2\rho)]^{1/2}\,, \tag{3}$$

where

$$D=[(C_{11}-C_{44})^2\cos^2 2\phi+(C_{12}+C_{44})^2\sin^2 2\phi]^{1/2}\,.$$

Here C_{11}, C_{12}, and C_{44} are the stiffness constants, ρ the mass density, and ϕ the angle between the y axis and the direction of propagation (Fig. 1). Equation (1) yields the velocity of a pure transverse wave polarized along the x axis (TA_x), Fig. 1. Equations (2) and (3) are quasitransverse (QT) and quasilongitudinal (QL) waves, respectively, and reduce to pure modes for special propagation directions. When $\phi=n\pi/4$ for integer n [of interest for (001)- and (011)-oriented GaAs/AlAs superlattices], all three modes are purely longitudinal or transverse [note that, in the (011) case, this is only valid in the continuum approximation]. For all other values of ϕ the $TA_{\perp x}$ and LA modes are mixed. This pattern is in agreement with the rule that there is no TA-LA mixing for propagation along a rotation axis of the point group. Thus, for the case of [012] propagation, $\phi=\cos^{-1}(1/\sqrt{5})=63.43°$, there are one pure transverse mode polarized along [100] and two mixed modes; the $[0\bar{2}1]$ TA mode is mixed with the [012] LA mode. The normal-mode polarization vectors for the wave speeds of Eqs. (1), (2), and (3) are, respectively,

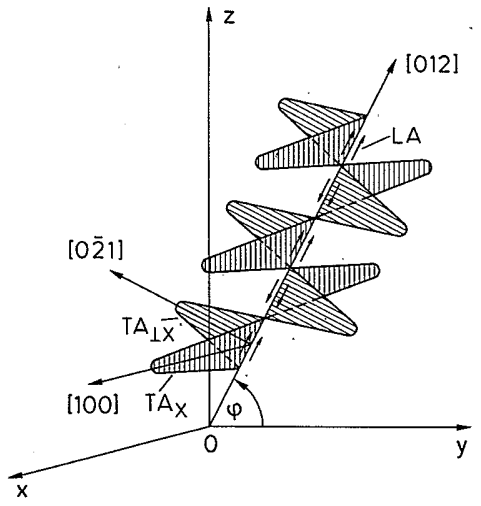

FIG. 1. Schematic representation of acoustic wave propagation along the [012] direction of a cubic crystal.

$$\hat{e}_T=\hat{e}_{[100]}\ , \tag{4}$$

$$\hat{e}_{QT}=N_T[(A-S)\hat{e}_{[0\bar{2}1]}+(B-2S)\hat{e}_{[012]}]\ , \tag{5}$$

$$\hat{e}_{QL}=N_L[(A+S)\hat{e}_{[0\bar{2}1]}+(B+2S)\hat{e}_{[012]}]\ , \tag{6}$$

where N_T, N_L are normalization constants, and

$$A=11C_{44}-3C_{11}+8C_{12}\ ,$$

$$B=2C_{44}-6C_{11}-4C_{12}\ ,$$

$$S=[9(C_{11}-C_{44})^2+16(C_{12}+C_{44})^2]^{1/2}\ .$$

Using the tabulated elastic moduli[3] of GaAs and AlAs, we determine the parameters of Table I for the [012] propagation direction. Note that the TA-LA amplitude admixture amounts to more than 10%. The square of the amplitudes, which determines the ratio of the TA to the LA Raman signals if only one of the two components is allowed, is mixed only at the 2% level.

In a superlattice there will be further mixing of modes 2 and 3 above, as a result of the differing acoustic properties of GaAs and AlAs. We will ignore this in what follows; the effects of this mixing are shown to be small below.

In order to determine the Raman selection rules for the folded acoustic phonons of superlattices in the elastic approximation, we must consider the selection rules given by the Brillouin tensors[4] of the bulk crystals. The coupling is through the periodic modulation of the optic polarizability in the presence of a phonon, and thus there is a finite cross section only if the strain of the phonon induces a change in the appropriate component of the susceptibility. The elasto-optic tensor has only three independent, but complex, components (p_{11}, p_{12}, and p_{44}) in cubic systems, analogous to the compliance tensor. In terms of these components, the phonon-modulated susceptibility tensors for $q=[012]/\sqrt{5}$ are

$$\frac{\epsilon_0^2}{\sqrt{5}}\begin{bmatrix}0 & p_{44} & 2p_{44}\\ p_{44} & 0 & 0\\ 2p_{44} & 0 & 0\end{bmatrix} \quad \text{for the TA}^{[100]}\text{ mode ,}$$

$$\frac{\epsilon_0^2}{5}\begin{bmatrix}0 & 0 & 0\\ 0 & 2(p_{12}-p_{11}) & -3p_{44}\\ 0 & -3p_{44} & 2(p_{11}-p_{12})\end{bmatrix} \quad \text{for the TA}^{[0\bar{2}1]}\text{mode ,}$$

$$\frac{\epsilon_0^2}{5}\begin{bmatrix}5p_{12} & 0 & 0\\ 0 & p_{11}+4p_{12} & 4p_{44}\\ 0 & 4p_{44} & p_{12}+4p_{11}\end{bmatrix} \quad \text{for the LA}^{[012]}\text{mode .}$$

The corresponding Brillouin polarization rules in the backscattering geometry for acoustic phonons in [012] GaAs/AlAs superlattices are given in Table II. Note that the only criterion used in constructing Table II is that there is an induced electric dipole moment (polarization) in the direction specified by the analyzer. Raman scattering from folded phonons will in fact be observed only if the polarization in the two layer types differs; this will of course occur as a result of differences in the two materials of both the normal-mode amplitude and the elasto-optic constants.[1] On the assumption that the bulk QT and QL modes are not very strongly mixed in the superlattice, the selection rules for TA and LA strains will also approximately apply to these modes.

The samples studied here are four GaAs/AlAs superlattices grown along the [012]-oriented undoped semi-insulating GaAs substrates by molecular-beam epitaxy. Details of the growth procedure and x-ray characterization of the samples studied, as well as a Raman study of optical phonons in these superlattices, are given in earlier papers.[5,6] The constituent layer thicknesses of the samples are represented by the number of GaAs (n_1) and AlAs (n_2) monolayers, each monolayer being 1.263 Å thick. The actual superlattice period of the samples was measured with a computer-controlled high-resolution double crystal x-ray diffractometer.[6] This procedure yielded the parameters $(n_1,n_2)=(21,25)$, (14,16), (23,8), and (6,42).

The Raman spectra were measured in the quasibackscattering geometry using a Spex Industries double monochromator (model 1404) with a conventional photon-counting detection system. The excitation

TABLE I. Velocities and polarizations of the three acoustic modes propagating along [012] of GaAs and AlAs. The polarization is given both as a ratio of longitudinal to transverse amplitude and as the square of the fraction of the displacement that is a result of longitudinal motion. It is this latter ratio that determines the strength of a Raman or Brillouin signal. These data were obtained from the elastic constants $c_{11}=11.84\times10^{11}$ dyn/cm^2, $c_{12}=5.37\times10^{11}$ dyn/cm^2, and $c_{44}=5.91\times10^{11}$ dyn/cm^2 for GaAs; and $c_{11}=12.5\times10^{11}$ dyn/cm^2, $c_{12}=5.34\times10^{11}$ dyn/cm^2, and $c_{44}=5.42\times10^{11}$ dyn/cm^2 for AlAs, as listed in Ref. 3.

Acoustic mode	v (10^5 cm/s)		$\frac{U_{\text{long}}}{U_{\text{trans}}}$		$\frac{(U_{\text{long}})^2}{(U_{\text{long}})^2+(U_{\text{trans}})^2}$	
	GaAs	AlAs	GaAs	AlAs	GaAs	AlAs
T	3.33	3.83				
QT	2.75	3.35	0.135	0.114	0.018	0.013
QL	5.08	6.1	7.42	8.71	0.982	0.987

TABLE II. The polarization selection rules in the backscattering geometry for acoustic phonons for GaAs/AlAs superlattices grown along the [012] direction as carried over from bulk crystal; $H=[100]$ and $V=[0\bar{2}1]$, and neglecting TA-LA admixture. p_{ij}, elasto-optic constants.

Configuration	Incident polarization	Scattering polarization	Scattering cross section TA [100]	TA [$0\bar{2}1$]	LA [012]
HH	[100]	[100]	0	0	p_{12}^2
HV	[100]	[$0\bar{2}1$]	0	0	0
VH	[$0\bar{2}1$]	[100]	0	0	0
VV	[$0\bar{2}1$]	[$0\bar{2}1$]	0	$[\frac{6}{25}(-p_{11}+p_{12}+2p_{44})]^2$	$[\frac{1}{25}(8p_{11}+17p_{12}-16p_{44})]^2$

sources were the 4579-, 4880-, and 5145-Å lines of Ar^+-ion laser and the 6471-Å line of a Kr^+-ion laser. Measurements were made in vacuum at room temperature.

Raman spectra of (21,25) and (14,16) superlattices in the spectral range between 10 and 120 cm^{-1} are shown in Fig. 2, and for (23,8) and (6,42), samples are shown in Fig. 3. The laser lines used in each case (see figure caption) correspond to nonresonant conditions.

Compatible with the selection rules of Table I, the QT- and QL-folded acoustic-phonon doublets are of similar strength for *VV* polarization, while in *HH* polarization the QL mode is nearly an order of magnitude larger than QT; the appearance of a weak QT doublet in *HH* polarization is due to mixing with the QL mode. In addition to the QT and QL doublets in Fig. 2(a), there are much weaker features between 23 and 30 cm^{-1}, and between 50 and 85 cm^{-1}. We assign a shoulder at about 25 cm^{-1} to a [100] TA mode, since its position is in reasonable agreement with the velocity of this branch (see Table I). This mode is actually forbidden by selection rules, but may be observed because the incident and scattered photons are not exactly along the [012] in quasibackscattering.

The next two peaks at 67 and 73 cm^{-1} correspond to the second QL doublet, and the broad feature at about 82 cm^{-1} to the TA mode of GaAs at the edge of the Brillouin zone (*X* point). For any one sample the asymmetry of the intensities observed for the two peaks is the same for the QT and QL doublets. It can be understood on the basis of the intensity analysis of folded phonons in (001) GaAs/AlAs superlattices (see Fig. 3.26 of Ref. 1); for (21,25) and (14,16) superlattices the parameter $\alpha=(d_{\mathrm{AlAs}}/d_{\mathrm{AlAs+GaAs}})$ is 0.54 and 0.53, respectively. For these values of α we can expect the -1 line to be somewhat stronger than the $+1$ line, and a very small intensity for the second folded QT and QL doublets.

In Fig. 3 the Raman spectra from samples with different GaAs and AlAs layer thicknesses are given. This asymmetry in layer thickness causes an asymmetry also in the intensities of the components of the QT- and QL-folded doublets. For the (23,8) superlattice the -1 line is twice as strong as the $+1$ line, and the opposite is true for the (6,42) superlattice. This is again in agreement with the analysis of [001] superlattices.[1] For (6,42) superlattices, besides QT and QL doublets, we clearly see the $+1$ line of the transverse-folded phonon branch in [100] direction; the absence of the -1 line of this doublet can be attributed to overlap with the $+1$ line of the QT doublet.

The layer thickness asymmetries of the (23,8) and (6,42) samples correspond rather closely to those for which the second-order folded doublets are strongest.[1] The absence of strong second-order signals may reflect superlattice period variations, although we note also that the second-order QL doublet would lie in a region (≈ 100 cm^{-1}), where the [$0\bar{2}1$] TA component no longer propagates in the GaAs layers. Moreover, for the (23,8) superlattice, we cannot resolve the second QT doublet, since it falls exactly at the position of the first QL-folded phonon doublet. In the case of the (6,42) superlattice, the second QT doublet falls somewhat lower than the first QL doublet, and the asymmetry of the -1 line of the QL doublet [Fig. 3(b) for *VV* polarization] can be explained as a superposition of the $+1$ line of the second QT doublet and the -1 line of the first QL doublet. In the Raman spectra of this sample there are two shoulders at about 80 and 104 cm^{-1}. The shoulder at about 80 cm^{-1} probably arises from superlattice and disorder-induced scattering by the [100] and [$0\bar{2}1$] TA acoustical branches of GaAs, which are practically flat for q between the *W* and *X* points of the [012] direction.[6] The same is true for the shoulder at about 105 cm^{-1} with regards to the dispersion relations of AlAs.

Finally, we compare the frequencies of the folded phonon doublets with predictions based on acoustic waves in the bulk. At the simplest level we use the average wave number $\bar{\nu}$ of the first-order doublets to obtain an estimate of the effective sound velocity:[1]

$$v_e = cd\bar{\nu} \ . \tag{7}$$

Here c is the speed of light, and d the period. The velocities found with Eq. (7) are, in all cases, in agreement with those obtained from the splitting ($\Delta\nu$) between the two components of the doublets, which are near 2.8 cm^{-1} for the QT and 5 cm^{-1} for the QL modes. In Table III we compare the speeds determined by Eq. (7) with the prediction[1]

$$\frac{d}{v_e}=\frac{d_1}{v_1}+\frac{d_2}{v_2} \ , \tag{8}$$

where d_i and v_i are the single-layer thicknesses and the sound velocities [Eqs. (2) and (3)] of material type i. Note

that for the (6,42) sample the disorder evident in the x-ray and optical confined phonon spectra[6] led to a large uncertainty in the thicknesses, and thus this sample has been omitted from Table III.

The speeds determined from the doublets are larger than the theoretical estimates [Eq. (8)] by 7 to 12% for the QL branch, and by −2 to 5% for the QT branch. The fact that the fractional disagreement differs for the two branches establishes that it is not simply due to an error in the superlattice period; it is the elastic constants used, probably those for AlAs, that are in error.

In order to include the effects of zone-center gaps and of QL-QT mixing in the superlattice, we have performed a continuum-model calculation, again based on the veloc-

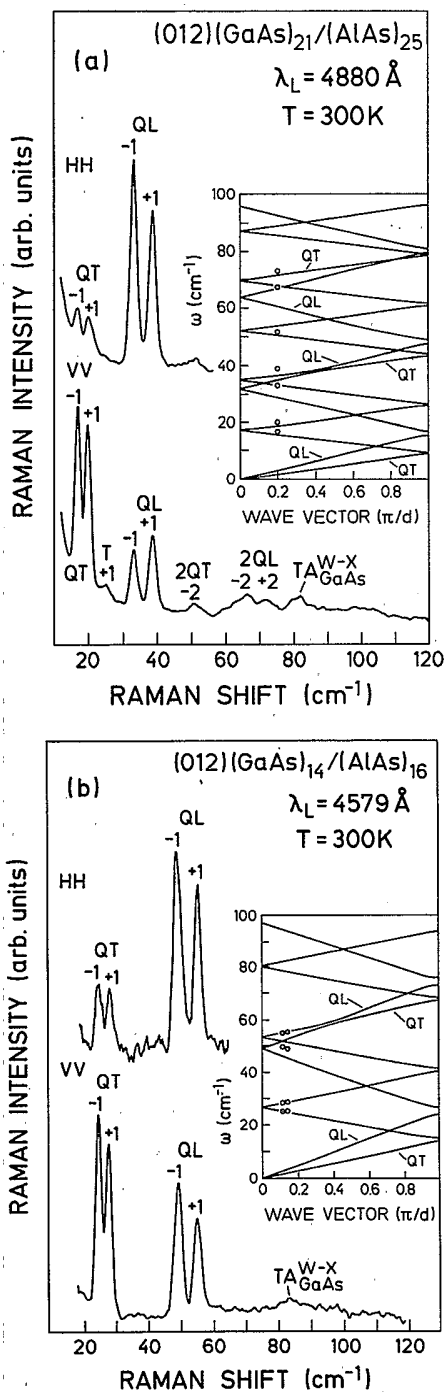

FIG. 2. Raman spectra of the (21,25) (a) and (14,16) (b) samples measured with 4880 and 4579 Å, respectively. The insets show continuum-model results for the QT- and QL-folded phonon-dispersion curves. Experimental values are denoted with open circles.

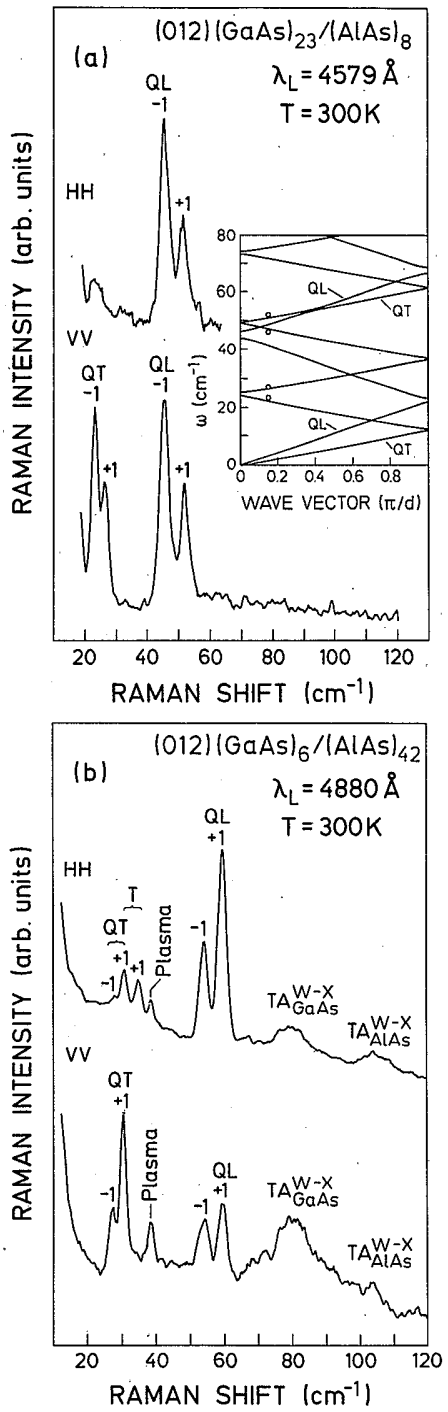

FIG. 3. Raman spectra of the (23,8) (a) and (6,42) (b) samples measured with 4579 and 4880 Å, respectively. The inset shows continuum-model results for the QT- and QL-folded phonon-dispersion curves together with experimentally observed folded phonons (open circles).

TABLE III. Measured [Eq. (7)] and calculated [Eq. (8)] effective speeds of the QT and QL waves in the superlattices. The fractional difference is quoted in the sense of measured minus calculated.

		v_e (10^5 cm/s)		
(n_1,n_2)	Branch	Measured (±3%)	Calculated	Fractional difference
(14,16)	QT	3.00	3.05	−2%
	QL	5.95	5.55	7%
(21,25)	QT	3.20	3.05	5%
	QL	6.35	5.60	12%
(23,8)	QT	3.05	2.90	5%
	QL	5.90	5.35	9%

ities and normal-mode vectors of Eqs. (2)–(6). The results are shown as insets in Figs. 2 and 3. Both the gaps and the effects of mixing can be seen in the dispersion curves, but these are weak and do not significantly alter the disagreement shown in Table III.

In the many reports of folded-acoustic-phonon measurements on (001) superlattices, there appears to be general agreement with the velocity given by Eq. (8). In this case only the longitudinal wave is detected, which for [001] propagation involves only one elastic constant (C_{11}). For [110] propagation, however, the LA wave speed involves all three constants; measurements made on a (110) sample[7] show agreement to within 2% between the results of Eqs. (7) and (8). It is possible that there are errors in the tabulated values of C_{12} and C_{44} for AlAs, and that these errors accidently cancel for the [110] LA velocity. These errors would have to be rather large, of the order of 30%, in order to explain a 10% error in the [012] QL velocity. Alternatively, the elastic constants in the (012)-superlattice layers may differ from those in the bulk and in (110) superlattices.[8]

We would like to thank H. Hirt, M. Siemers, and P. Wurster for expert technical help, and L. Tapfer for the x-ray characterization of the samples. Z.V.P. acknowledges financial support from the Alexander von Humboldt Foundation.

*Permanent address: Institute of Physics, P.O. Box 57, YU-11000 Belgrade, Yugoslavia.

†Permanent address: Department of Physics, Victoria University of Wellington, Wellington, New Zealand.

[1]B. Jusserand and M. Cardona, in *Light Scattering in Solids V*, edited by M. Cardona and G. Güntherodt (Springer-Verlag, Heidelberg, 1989), p. 49.

[2]B. A. Auld, *Acoustic Fields and Waves in Solids* (Wiley, New York, 1973), Vol. 1, p. 191.

[3]*Physics of Group IV Elements and III-V Compounds,* Vol. 17a of *Landolt-Börnstein Tables,* edited by O. Madelung (Springer, Berlin, 1982), p. 235.

[4]H. Z. Cummins and P. E. Schoen, in *Laser Handbook,* edited by F. T. Arecchi and E. O. Schulz-Dubois (North-Holland, Amsterdam, 1972), p. 1029.

[5]Z. V. Popović, M. Cardona, L. Tapfer, K. Ploog, E. Richter, and D. Strauch, Appl. Phys. Lett. **54**, 846 (1989).

[6]Z. V. Popović, M. Cardona, E. Richter, D. Strauch, L. Tapfer, and K. Ploog, following paper, Phys. Rev. B **40**, 1207 (1989).

[7]Z. V. Popović, M. Cardona, E. Richter, D. Strauch, L. Tapfer, and K. Ploog, Phys. Rev. B (to be published).

[8]M. H. Grimsditch, in Ref. 1, p. 285.